Computer Assisted Methods in Engineering and Science
32(2): 179–211, 2025, https://doi.org/10.24423/cames.2025.1783

43rd SolMech 2024

Pattern-Based Approach to Topology and Geometry Optimization of Steel Building Structures

Artur LAX[1)*], Sławomir MILEWSKI[2)]

[1)] *Doctoral School, Cracow University of Technology, Cracow, Poland*

[2)] *Chair for Computational Engineering, Faculty of Civil Engineering, Cracow University of Technology, Cracow, Poland*

[*] *Corresponding Author e-mail: arturlax@hotmail.com*

This research primarily focuses on evaluating the effectiveness of various methodologies for the topological and geometrical optimization of steel building structures through parametric descriptions. The study specifically addresses steel trusses, frames, and beams, emphasizing their integration within the broader structural system. Initial investigations have highlighted the benefits of an innovative pattern-based approach that segments the structure into distinct patterns, namely groups of structural elements subjected to localized optimization. This method effectively overcome the challenges of global parameter optimization, by providing enhanced control over local criteria and enabling a more detailed assessment of each pattern's contribution to global optimization objectives. Building on these insights, the research seeks to advance and refine the concept of patterns, aiming to further enhance their applicability and efficiency in structural optimization.

Keywords: topological optimization, geometrical optimization, parametric description, steel structures, finite element method.

1. Introduction

1.1. Motivation

One of the fundamental challenges faced by structural designers is determining the optimal geometry and topology of steel structures, a task that becomes increasingly intricate as the number of structural elements grows. Moreover, identifying the geometric configuration that yields an optimal solution is often far from straightforward.

Traditionally, designers rely on an initial structural topology based on prior experience, followed by the design of cross-sections within this predefined con-

figuration. While practical, this approach excludes topology optimization as a fully integrated aspect of the design process. To overcome this limitation, multi-parametric and multi-criteria optimization can be incorporated into the workflow, enabling a more advanced and holistic design methodology.

Parametrizing the structural configuration facilitates global optimization, aiding in the identification of optimal solutions. However, as the number of parameters and criteria increases and the diversity of potential topologies expands, the computational complexity of the optimization problem grows significantly. This escalating complexity often presents a significant barrier to developing efficient optimization strategies.

Given these challenges, there is a pressing need for innovative approaches that combine efficiency with adaptability to meet the demands of designing complex steel structures. Such approaches should aim to improve the optimization process while maintaining the flexibility required to accommodate a wide range of structural configurations and criteria.

1.2. State-of-the-art

In the field of structural optimization, recent advancements have introduced a variety of classification systems, notably those proposed by Rozvany [1,2]. Rozvany's framework identifies three primary categories in structural optimization: layout optimization (LO), generalized shape optimization (GSO), and a hybrid approach combining both (LO+GSO) for composite structures. LO emphasizes optimizing grid-like bar structures in parallel, while GSO primarily addresses plane stress problems. In addition, Sigmund [3] has provided a comprehensive review of these and other optimization techniques, contributing to a broader understanding of their applicability and limitations.

Several commercial software tools support parametric design and structural optimization, including Grasshopper 3D, CATIA, Dynamo, and Altair OptiStruct. These tools are particularly efficient for global optimization and often implement or support the GSO approach.

Topology optimization for steel structures has been extensively studied, with various methodologies tailored to specific challenges [4, 5]. The optimization of bar structures typically involves a multi-dimensional, single-objective problem characterized by constraints and decision variables of mixed numerical types, such as Boolean, integer, and real values. To manage this complexity both stochastic and deterministic strategies have been developed.

Stochastic approaches include:

– genetic algorithms [6] and other biologically inspired methods [7],
– Monte Carlo simulations [8, 9].

Deterministic methods feature:

- non-gradient approaches such as joint penalty methods with material selection [10],
- gradient-free proportional optimization techniques [11],
- techniques incorporating buckling constraints for spatial trusses [12].

Additionally, gradient-based approaches, such as non-smooth steepest descent algorithms [13], have proven effective in tackling such problems.

For instance, a genetic algorithm has been proposed to optimize steel truss roofs, integrating structural constraints and offering a framework applicable to various structural forms [14]. Another study combined shape and cross-section optimization for planar trusses, unifying stress and geometrical constraints within a single framework. Using a full stress design and conjugate gradient optimization, this approach demonstrated significant material savings, drawing comparisons to steel bridge designs of the early 20th century [15].

To address large-scale truss optimization, innovative methods have been introduced:

- The cooperative coevolutionary marine predators algorithm (CCMPA-GS), which optimizes shape and size separately in a multi-modal search space, demonstrating superior scalability and performance compared to traditional methods [16].
- The dual-material truss bidirectional evolutionary structural optimization (DMT-BESO) method integrates topology and size optimization while utilizing materials with distinct tensile and compressive properties. By incorporating structural complexity control strategies, this method enhances material utilization while ensuring compliance to industry standards [17].

Steel grillage structures were optimized using SAP-Rao algorithms to minimize weight while satisfying stress and displacement constraints. The method was validated through FEM and MATLAB, proving its effectiveness for structural design [18]. The Jaya algorithm was applied to optimize truss structures, focusing on weight reduction by adjusting shape and size variables. Its simplicity and efficiency were demonstrated through MATLAB-based FEM analysis and benchmark case studies [19]. Novel techniques, such as the numerical inverse hanging method, which have been introduced to optimize spatial trusses by improving load-bearing capacity and stability under varying boundary conditions. This approach provides a robust framework to address form-finding challenges in spatial truss design, expanding topology optimization to complex geometries [20].

The contributions of Kaveh to structural optimization are particularly notable, especially in developing innovative algorithms for design. Key examples include:

- The imperialist competitive algorithm (ICA) models optimization as a socio-political competition among empires, yielding effective solutions for trusses and frames [21].
- The hybrid Big Bang–Big Crunch (HBB–BC) algorithm has been applied to truss size optimization, outperforming other heuristic methods such as genetic algorithms, ant colony optimization, and particle swarm optimization [22].
- More recently, the sequential optimization and reliability assessment-double meta-heuristic (SORA-DM) approach has been utilized for reliability-based design optimization (RBDO) of frame structures, incorporating enhanced algorithms such as the shuffled shepherd optimization algorithm (SSOA) for improved performance [23].

While these methodologies effectively address individual challenges through global parameters, they often lack the granularity required for precise optimization of specific components within a structural system. A versatile approach that can be seamlessly applied to various structural systems is essential to enhance design efficiency. Without such an approach, defining a comprehensive optimization problem for an entire structure can become inefficient and overly time-consuming. Although truss topology optimization has been extensively studied, mixed systems involving frames and trusses – commonly encountered in real-world design tasks – remain underexplored.

1.3. The concept of patterns

This study builds upon and further refines the concept of structural patterns introduced in the authors' previous research [24]. The methodology is based on the principle that a structure can be divided into distinct patterns – sets of structural elements, which significantly reduces the number of decision variables. By focusing on localized optimization tasks within these patterns, the complexity of global-level analysis is minimized, enabling a more efficient and reliable optimization process.

Structural patterns are designed to facilitate the formulation of separate optimization problems with fewer variables, making the process computationally manageable. Design parameters associated with these patterns are subsequently optimized using deterministic or stochastic algorithms. The choice of algorithm depends on factors such as solution accuracy, computational efficiency, the availability of gradients, and problem complexity. Once optimized, these localized patterns are integrated into a global framework, ensuring that interactions between patterns are appropriately addressed.

This approach is highly versatile, enabling the simultaneous optimization of structural and architectural parameters while also considering economic fac-

tors, such as material usage, and engineering criteria, such as compliance with limit states. This provides a robust framework for tackling single- or multi-criteria nonlinear optimization problems, offering both computational efficiency and practical applicability in structural design.

The results presented in this study were obtained using proprietary prototype software developed by the authors, primarily implemented in C++ and MATLAB. Visualization and plotting were facilitated using the Python Matplotlib library. The genetic algorithm implementations were supported by the MATLAB Global Optimization Toolbox and the esa-pagmo2 C++ library [25].

The paper is structured as follows:

- Section 2 provides an overview of the formulation for multidimensional and multi-objective optimization problems,
- Section 3 discusses the foundational principles of the computational approaches used, with a particular focus on integrating structural patterns into optimization algorithms,
- Section 4 presents the results of selected engineering optimization case studies involving parametrically described structures,
- Section 5 concludes the paper with a summary of findings and recommendations for future research directions.

2. Formulation of the optimization problem

The optimization problem is defined using a vector of decision variables $\mathbf{d} = [\mathbf{b}, \mathbf{z}, \mathbf{r}]$, where $\mathbf{b}$ represents n_b Boolean variables, $\mathbf{z}$ represents n_z integer variables, and $\mathbf{r}$ represents n_r real variables. In the case of steel bar structures, these variable types are used to comprehensively describe both topology and geometry parameters. For instance, integer variables may define the number of bars, nodes, supports, levels, or naves, Boolean variables may indicate the existence of specific bars or supports, and real variables may describe bar lengths or parameters of their cross-sections. Thus, the total number of decision variables is $n_d = n_b + n_z + n_r$. The multidimensional objective function, $\mathbf{F}(\mathbf{d}) = [F_1(\mathbf{d}), ..., F_{n_f}(\mathbf{d})]$, is based on multiple criteria, such as maximum displacement, bending moments, reaction forces, critical forces, eigenfrequencies, or material usage. Computing the components of $\mathbf{F}(\mathbf{d})$ requires solving the boundary value problem for the bar structure with a temporarily fixed set of decision variables. Moreover, some objectives may involve solving local optimization problems or performing simplified evaluations at predefined structural points to ensure accuracy and efficiency in the analysis.

The admissible domain Ω_{adm} is defined by the bounds applied to the decision variables:

$$\Omega_{\text{adm}} = \left\{ b_i \in \{0,1\},\ \ z_j \in [z_j^{\min}, z_j^{\max}],\ \ r_k \in [r_k^{\min}, r_k^{\max}] \right\}, \tag{1}$$

where $i = 1, ..., n_b$, $j = 1, ..., n_z$, and $k = 1, ..., n_r$. Here, $z_j^{\min}$, $z_j^{\max}$, $r_k^{\min}$, and $r_k^{\max}$ represent the prescribed limits imposed on the integer and real variables, respectively.

Additional constraints, both equality and inequality, are expressed as:

$$\mathbf{R}_{\text{eq}}(\mathbf{d}) = 0, \qquad \mathbf{R}_{\text{ineq}}(\mathbf{d}) < 0, \tag{2}$$

which help define the optimization problem. In this research, the focus is on linear equality constraints, which can be incorporated into the optimization problem using either the elimination technique – thereby reducing the number of decision variables – or Lagrange multipliers, which increase the number of unknowns.

In contrast, inequality constraints, which typically require specialized numerical treatment (e.g., using the feasible directions method), are omitted in favor of a multi-objective optimization framework. This approach allows additional limitations to be imposed in an alternative manner, thus avoiding the complexity associated with traditional inequality constraints.

2.1. Single-objective optimization

In single-objective optimization, the multidimensional objective function simplifies to a scalar function ($n_f = 1$), which depends on at least one real decision variable ($n_d \geq n_r \geq 1$). The optimization problem is formulated as:

$$\min_{(\mathbf{d})} F(\mathbf{d}) \quad \text{for} \quad \mathbf{d} \in \Omega_{\text{adm}}. \tag{3}$$

The optimal solution to this problem is expressed as:

$$\mathbf{d}^{(\text{opt})} = \arg\min_{(\mathbf{d})} F(\mathbf{d}), \tag{4}$$

where the existence of a solution is ensured by the Kuhn–Tucker conditions. For unconstrained problems, these conditions require:

1. The gradient of the objective function to vanish:

$$\boldsymbol{\nabla}_{\mathbf{d}} F(\mathbf{d}) = \mathbf{0}. \tag{5}$$

2. The Hessian matrix:

$$\mathbf{H}(\mathbf{d}) = \boldsymbol{\nabla}_{\mathbf{d}} \otimes \boldsymbol{\nabla}_{\mathbf{d}} F(\mathbf{d}) \tag{6}$$

to be positive definite.

The positive definiteness of the Hessian ensures the convexity of the function. This convexity is essential for compatibility with deterministic optimization methods and guarantees the existence of a unique local minimum.

2.2. Multi-objective optimization

In multi-objective optimization ($n_f > 1$), conflicting criteria make it impossible to achieve simultaneous minimization of all objectives. A solution $\mathbf{d}_j$ is said to dominate $\mathbf{d}_k$, namely the following symbolic relationship is valid:

$$F_l(\mathbf{d}_j) \leq F_l(\mathbf{d}_k) \quad \forall l \quad \text{and} \quad \exists l \text{ such that } F_l(\mathbf{d}_j) < F_l(\mathbf{d}_k), \tag{7}$$

providing the following conditions are satisfied:

1. $F_l(\mathbf{d}_j) \leq F_l(\mathbf{d}_k)$ for all $l = 1, ..., n_f$, and
2. $F_l(\mathbf{d}_j) < F_l(\mathbf{d}_k)$ for at least one l.

This concept of dominance leads to the definition of a Pareto front, which consists of all non-dominated solutions. Each point on the Pareto front represents a trade-off between competing objectives, offering decision-makers a set of equally optimal solutions from which to choose based on specific priorities or preferences.

Methods to address multi-objective problems include:

– weighted average method: this approach solves n_f single-objective problems and then combines their results:

$$\mathbf{d}^{(\text{opt})} \approx \sum_{l=1}^{n_f} \omega_l \mathbf{d}_l^{(\text{opt})}, \text{ with non-negative weights such that } \sum_{l=1}^{n_f} \omega_l = 1; \tag{8}$$

– ε-constrained method: here one objective is optimized while the constrained others are prescribed with ε_l tolerances:

$$\min_{(\mathbf{d})} F_i(\mathbf{d}), \qquad F_l(\mathbf{d}) \leq \varepsilon_l; \tag{9}$$

– weighted sum method: this method scalarizes multiple objectives into a single objective function:

$$F(\mathbf{d}) = \sum_{l=1}^{n_f} \omega_l F_l(\mathbf{d}), \text{ with non-negative weights such that } \sum_{l=1}^{n_f} \omega_l = 1; \tag{10}$$

– weighted metric method: it minimizes the distance from the ideal solution using the p-norm:

$$\min_{(\mathbf{d})} L_p(\mathbf{d}), \qquad L_p(\mathbf{d}) = \left(\sum_{l=1}^{n_f} \omega_l \left| F_l(\mathbf{d}) - F_l^{(\text{opt})} \right|^p \right)^{1/p}. \tag{11}$$

Each optimization method has its unique advantages and limitations. Techniques such as weighted metrics, for example, are particularly effective for identifying Pareto-optimal fronts, even in non-convex spaces. Other approaches offer flexibility by allowing to emphasize specific objectives through weight assignment,

making them robust tools for navigating the trade-offs inherent in multi-objective optimization problems.

In this study, two approaches were employed based on the problem formulation. For multi-objective problems, a Pareto-based optimization strategy was used to generate a set of non-dominated solutions. In contrast, for single-objective problems derived from multiple objectives, the weighted sum method was applied to aggregate the objectives into a single scalar function.

3. Computational approaches

The absence of an explicit analytical form for the objective function necessitates the use of numerical methods to compute its values and derivatives. Both the optimization problems and the auxiliary boundary value problems associated with these numerical approaches require the application of diverse computational techniques. In this context, numerical frameworks such as the finite element method (FEM), specifically in its displacement formulation play a crucial role. FEM enables the analysis of deformation states based on the design variables $\mathbf{d}$ generated during the optimization process, thereby providing accurate and reliable insights into the structural behavior under various conditions.

3.1. Finite element model

The structural optimization conducted in this study employed FEM. The analysis utilized a combination of various element types to accurately model the structural components. These included frame elements, truss bar elements, and spring interface units, each tailored to effectively represent the corresponding structural behavior and interactions. The following types of local stiffness matrices are incorporated within the numerical framework:

– 2D frame bars were modeled using the Timoshenko beam theory, which accounts for shear deformations [26]. The stiffness matrix for a 2D frame element is expressed as:

$$\mathbf{K}_{\text{frame}}(\mathbf{d}) = \begin{bmatrix} \frac{12I(\mathbf{d})E}{L^3(\mathbf{d})} & 0 & 0 & -\frac{12I(\mathbf{d})E}{L^3(\mathbf{d})} & 0 & 0 \\ 0 & \frac{A(\mathbf{d})E}{L(\mathbf{d})} & \frac{6I(\mathbf{d})E}{L^2(\mathbf{d})} & 0 & -\frac{A(\mathbf{d})E}{L(\mathbf{d})} & \frac{6I(\mathbf{d})E}{L^2(\mathbf{d})} \\ 0 & \frac{6I(\mathbf{d})E}{L^2(\mathbf{d})} & \frac{4I(\mathbf{d})E}{L(\mathbf{d})} & 0 & -\frac{6I(\mathbf{d})E}{L^2(\mathbf{d})} & \frac{2I(\mathbf{d})E}{L(\mathbf{d})} \\ -\frac{12I(\mathbf{d})E}{L^3(\mathbf{d})} & 0 & 0 & \frac{12I(\mathbf{d})E}{L^3(\mathbf{d})} & 0 & 0 \\ 0 & -\frac{A(\mathbf{d})E}{L(\mathbf{d})} & -\frac{6I(\mathbf{d})E}{L^2(\mathbf{d})} & 0 & \frac{A(\mathbf{d})E}{L(\mathbf{d})} & -\frac{6I(\mathbf{d})E}{L^2(\mathbf{d})} \\ 0 & \frac{6I(\mathbf{d})E}{L^2(\mathbf{d})} & \frac{2I(\mathbf{d})E}{L(\mathbf{d})} & 0 & -\frac{6I(\mathbf{d})E}{L^2(\mathbf{d})} & \frac{4I(\mathbf{d})E}{L(\mathbf{d})} \end{bmatrix}, \quad (12)$$

where $I(\mathbf{d})$ denotes the moment of inertia, $L(\mathbf{d})$ is the element length, E represents the modulus of elasticity, and $A(\mathbf{d})$ is the cross-sectional area. This formulation provides the foundation for analyzing frame behavior under deformation while considering both bending and shear effects.

– 2D truss elements are designed to carry axial forces exclusively and are represented using the following stiffness matrix:

$$\mathbf{K}_{\text{truss}}(\mathbf{d}) = \frac{A(\mathbf{d})E}{L(\mathbf{d})} \begin{bmatrix} 1 & -1 \\ -1 & 1 \end{bmatrix}. \tag{13}$$

This matrix formulation accounts for the axial stiffness of truss elements and ensures that these elements only resist forces along their longitudinal axes. It forms a critical component of the overall FEM, particularly when combined with frame and spring elements to analyze complex structural systems.

– To model interaction between patterns, spring elements are utilized at the interfaces. These elements were characterized by their own stiffness matrix, which accounts for both translational and rotational stiffness properties. The stiffness values in the matrix are derived based on the displacements and rotations at the nodes, as well as the corresponding forces and moments. The stiffness matrix for the spring elements is expressed as:

$$\mathbf{K}_{\text{spring}}(\mathbf{d}) = \begin{bmatrix} k_x(\mathbf{d}) & 0 & 0 & -k_x(\mathbf{d}) & 0 & 0 \\ 0 & k_y(\mathbf{d}) & 0 & 0 & -k_y(\mathbf{d}) & 0 \\ 0 & 0 & k_\theta(\mathbf{d}) & 0 & 0 & -k_\theta(\mathbf{d}) \\ -k_x(\mathbf{d}) & 0 & 0 & k_x(\mathbf{d}) & 0 & 0 \\ 0 & -k_y(\mathbf{d}) & 0 & 0 & k_y(\mathbf{d}) & 0 \\ 0 & 0 & -k_\theta(\mathbf{d}) & 0 & 0 & k_\theta(\mathbf{d}) \end{bmatrix}, \tag{14}$$

where $k_x(\mathbf{d})$, $k_y(\mathbf{d})$, and $k_\theta(\mathbf{d})$ are the translational stiffness in the x-direction, the translational stiffness in the y-direction, and the rotational stiffness, respectively. These spring elements facilitate the interaction between structural patterns by transmitting forces and moments across their connections. Their inclusion ensures that the global system behavior accurately reflects the interactions between locally optimized patterns, thereby enhancing their robustness and accuracy of the overall structural model.

The global stiffness matrix for the structure, $\mathbf{K}(\mathbf{d})$, was assembled following the standard FEM formulation. The equilibrium equation governing the structural response is given as:

$$\mathbf{K}(\mathbf{d})\mathbf{Q} = \mathbf{P}(\mathbf{d}), \tag{15}$$

where $\mathbf{K}(\mathbf{d})$ represents the stiffness matrix, which is a function of the decision variables $\mathbf{d}$. The vector $\mathbf{Q}$ denotes the generalized nodal displacements, while $\mathbf{P}(\mathbf{d})$ is the load vector. Although the external load acting on the structure remains constant, the resulting discrete load vector $\mathbf{P}$ depends on the decision variables $\mathbf{d}$. Changes in geometry and topology affect the finite element discretization and the corresponding equivalent nodal loads, thus requiring updates to $\mathbf{P}$ during optimization.

The integration of frame, truss, and spring elements allowed for the detailed modeling of both individual components and their interactions within the overall structure. By utilizing the FEM framework, the study ensured that both the local and global structural responses were accurately captured, thereby facilitating an efficient and precise optimization of individual patterns and their contributions to the global system.

3.2. Optimization methods

Two optimization methods were utilized in this study: a direct search method and a genetic algorithm. These methods were applied to solve both single- and multi-objective optimization problems, with the aim of identifying optimal structural configurations and approximating the Pareto front. The direct search method, commonly referred to as brute force, was primarily employed for obtaining preliminary results. This method involved evaluating the objective function for all feasible combinations of decision variables within predefined bounds. Although computationally expensive, it served as a valuable reference for validating the optimization process and exploring the solution space, particularly for smaller-scale problems [24]. The primary optimization tool was a genetic algorithm, implemented using the MATLAB Global Optimization Toolbox and the pagmo2 library [25]. This approach was central to the study, enabling the efficient exploration of complex solution spaces and the identification of optimal designs. This research primarily focuses on the implementation and validation of the patterns-based approach for structural optimization. The integration of more sophisticated and advanced algorithms is planned as part of future research endeavors, further enhancing the potential of this methodology.

3.3. Implementation of patterns

The proposed methodology is based on dividing a selected building structure into characteristic patterns, each made up of specific sets of elements. This study focuses on several types of patterns, such as trusses and frames, which interact within the overall structure. These patterns can be assembled using various element types, offering a flexible and versatile approach to structural

modeling and optimization. Collectively, these patterns form the complete structure subjected to the optimization process. To facilitate efficient data exchange and seamless interaction between patterns, an object-oriented programming approach is employed. This design ensures modularity and adaptability in managing the relationships and dependencies among patterns. A general optimization algorithm, illustrated in Fig. 1, was developed based on this pattern-based methodology, providing a structured framework for solving complex structural optimization problems.

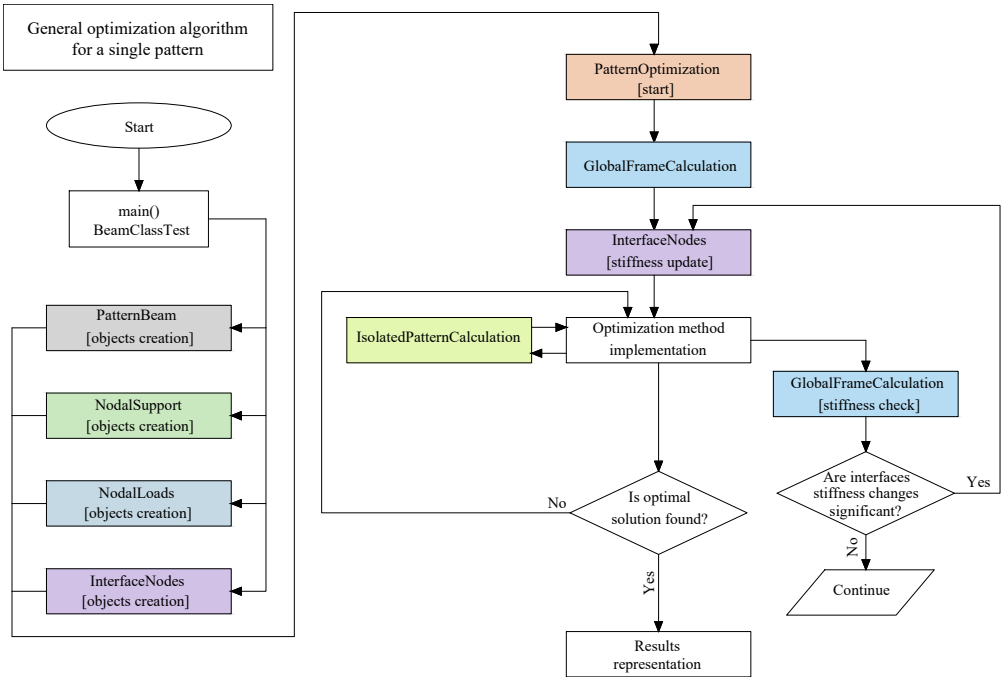

FIG. 1. General flowchart of pattern-based optimization algorithm.

The algorithm aggregates objective function values from individual patterns, to construct global objective functions. Patterns can also be optimized in isolation to facilitate local optimization. The process begins by creating of objects for all components of the structure, including patterns, supports, loads, and interfaces between patterns. These objects encapsulate all relevant information, such as stiffness matrices, loads, and connectivity details. The optimization process uses this information to perform both local optimization of individual patterns and global optimization of the entire structure. Additionally, the algorithm incorporates a mechanism to determine whether a pattern can be optimized in isolation without requiring a global solution update. This is decided by evaluating whether changes in the stiffness of the interfaces between patterns significantly

affects the forces in the global system. If the stiffness changes are negligible, local optimization can proceed without recalculating the global solution, which significantly improves computational efficiency. However, if each iteration requires stiffness updates, local optimization becomes ineffective, and global optimization remains the only viable approach.

The optimization process can evaluate objective function values (such as mass of elements) independently for each pattern. These values are then aggregated to define the global objective function. Specifically, the global objective vector $\mathbf{F}_{\text{tot}}$ is defined as:

$$\mathbf{F}_{\text{tot}} = \sum_{i=1}^{n_p} \mathbf{F}_i, \tag{16}$$

where n_p is the number of patterns, and $\mathbf{F}_i$ denotes the vector of objective function values associated with i-th pattern. This formulation supports localized evaluation while preserving global control over the optimization objectives.

For scalar objective functions, this summation reduces to a component-wise operation across all patterns. In multi-objective settings, the vector structure of $\mathbf{F}_{\text{tot}}$ is retained, allowing it to be directly applied in Pareto-based optimization or scalarization techniques such as the weighted sum method.

The following admissibility criteria were implemented to determine whether such decoupling is permissible:

– Relative change in global internal force response must remain within acceptable limits, as it directly influences the local verification of elements:

$$\Delta f = \frac{\left\|\mathbf{N}^{(i+1)} - \mathbf{N}^{(i)}\right\|}{\left\|\mathbf{N}^{(i)}\right\|} < \varepsilon_f, \qquad \text{and similarly for } \mathbf{V},\, \mathbf{M}; \tag{17}$$

– Relative change in interface stiffness is monitored but is not treated as a strict condition in this study:

$$\Delta k = \frac{|k_x^{(i+1)} - k_x^{(i)}|}{k_x^{(i)}} < \varepsilon_k, \qquad \text{and similarly for } k_y,\, k_\theta; \tag{18}$$

– The global stiffness sensitivity may also be evaluated using the Frobenius norm, although it is not the primary admissibility criterion:

$$\Delta K = \frac{\|\mathbf{K}^{(i+1)} - \mathbf{K}^{(i)}\|_F}{\|\mathbf{K}^{(i)}\|_F} < \varepsilon_K. \tag{19}$$

In practice, local optimization is allowed to proceed as long as the change in internal forces remains within acceptable limits. While interface stiffness variations are monitored, the internal force response is treated as primary admissibility criterion, as it directly impacts the local verification of structural elements.

This focus reflects typical engineering procedures, where internal forces form the basis for design and safety checks. As a result, local optimization can be carried out without requiring full stiffness updates, enabling a computationally efficient decoupling of the local and global optimization stages.

Computational examples illustrating the application of this methodology are presented in the subsequent section.

4. Numerical examples

This study explores the application of pattern-based, object-oriented techniques in structural optimization, with a particular focus on their integration into finite element modeling workflows. Rather than relying on traditional monolithic modeling, the proposed approach leverages modular components–referred to as patterns–connected through interface elements. Implemented in C++, this framework enables flexible handling of design variables and structural configurations while offering potential computational benefits. The methodology is tested on several case studies, each addressing different aspects of structural optimization, including topology, parameter type, and structural decomposition.

Example 4.1 presents a classical optimization case involving two topological variants and integer parameters with practical engineering implementation. Example 4.2 introduces preliminary testing of frame decomposition using the object-oriented interface approach. Example 4.3 extends classical optimization to a larger topology space-featuring up to 36 integer-type parameters for the vertical bracings layout of the structure. Example 4.4 outlines a general concept for connecting multiple structural patterns.

In all presented examples, the optimization problems are formulated as minimization problems. Buckling effects and geometric nonlinearity were not considered in this study, as the focus was on evaluating the proposed optimization approach under simplified small-deformation conditions. This enabled the assessment of internal force- and moment-based objectives within a controlled framework. These aspects are intended to be addressed in future research, which will extend the methodology to include large-deformation analysis and buckling-related criteria.

The benchmarks were performed on a single thread of the Apple M3 Pro chip.

4.1. Steel tower optimization

To implement the developed computational approaches, a steel tower structure was designed using an isolated vertical truss pattern optimized via a genetic algorithm (Fig. 2). The tower acts as a supporting structure for a conveyor

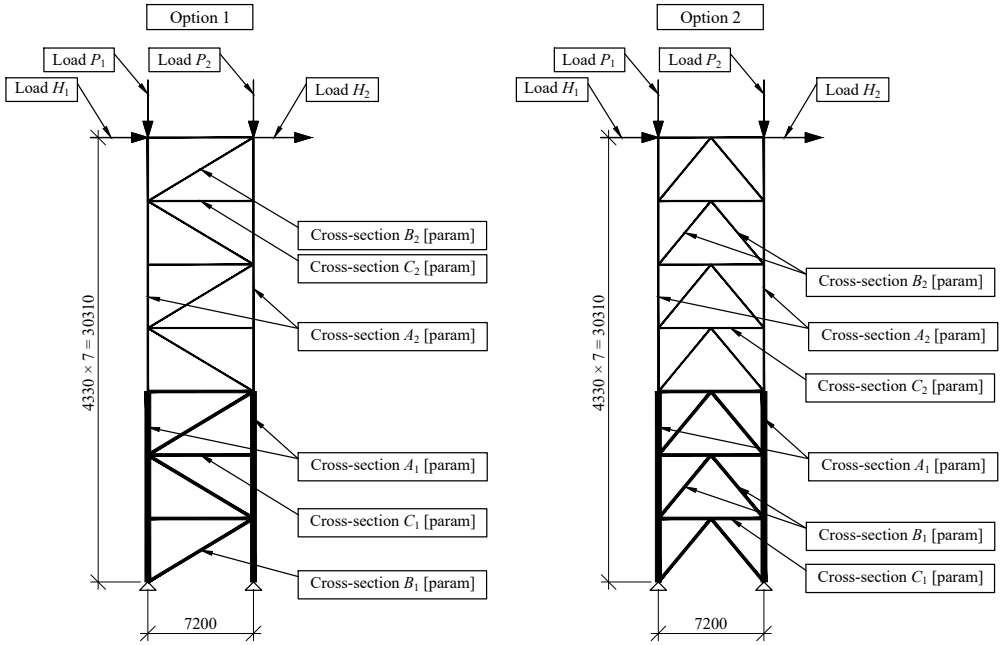

FIG. 2. Optimization scheme.

system. This example demonstrates how the proposed pattern-based approach applies to basic truss structures, which are defined by standard engineering parameters such as cross-sectional areas and truss widths, and have two possible topological configurations. Although the optimization procedure in this case follows a classical, monolithic approach without decomposition or interface modeling, the vertical truss structure serves as a representative pattern class within the proposed framework. This example illustrates how the internal features of a pattern – such as the configuration of its bracings – can be parametrized and optimized. This enables to reuse parametrically defined structural units for composing more complex systems, where interface conditions between patterns become relevant.

The applied loads consist of concentrated vertical forces $P_1 = P_2 = -100$ kN and horizontal forces $H_1 = H_2 = 40$ kN. The optimization problem considers a total of eight decision variables: seven real-type variables and one integer-type variable, represented as $\mathbf{d} = [A_1, A_2, B_1, B_2, C_1, C_2, W, T]$. The variables and their bounds are defined as follows:

- cross-sectional areas of elements (real):
  A_1, A_2, B_1, B_2, C_1, $C_2 \in [0.001, 0.1]$ m^2,
- width of the truss (real): $W \in [5, 12]$ m,
- type of bracings (integer): $T \in [1, 2]$.

Two optimization criteria were considered:

1. Displacement limitation, defined as the difference between the displacement at a control node and the admissible displacement:

$$F_1(\mathbf{d}) = |h(\mathbf{d}) - h_{\text{adm}}|, \qquad h_{\text{adm}} = \frac{\text{H}}{500}, \tag{20}$$

   where H represents the height of the vertical truss.
2. Steel usage, calculated as the total mass of the truss bars:

$$F_2(\mathbf{d}) = \sum_{i=1}^{n} A_i(\mathbf{d})\, l_i(\mathbf{d})\, \rho, \tag{21}$$

   where $A_i(\mathbf{d})$ and $l_i(\mathbf{d})$ denote the cross-sectional area and length of element i, respectively, and ρ is the material density. The total number of elements n depends on the geometry/topology of the scheme.

In this example, a scalarized optimization approach was used based on a mixed weighted criterion combining the two objectives: displacement control and steel usage. Rather than generating a full Pareto front, a fixed weighting was applied to balance these competing goals within a single objective function. This approach reflects a practical engineering design scenario where priorities between criteria are predefined.

Optimization results:

1. The algorithm consistently favored the upper limit of the admissible truss width.
2. Truss topology type 2 resulted in a weight reduction of 17% compared to topology type 1 in all scenarios.
3. In approximately 50% of optimization runs from different genetic algorithm starting points, configuration 2 was selected.
4. Configuration 2 utilized smaller cross-sections than configuration 1, which, in contrast, included a greater number of elements and nodes.
5. Horizontal bars had a negligible effect on the overall displacements.

To provide additional insight into the behavior of the objective function, two illustrative brute-force plots are presented in Figs. 3a and 3b. These plots show the shape of the objective function landscape for two selected parameters, helping to visualize the trade-off structure and confirm the presence of multiple optima. It should be emphasized that these graphs were generated solely for visualization purposes and do not represent the main optimization process, which was conducted using a genetic algorithm over a higher-dimensional design space.

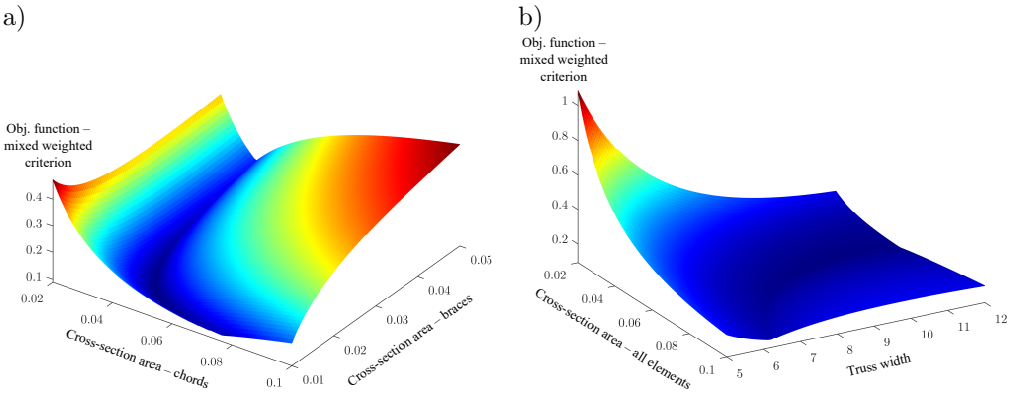

FIG. 3. Graphs illustrating the objective function values for the vertical truss, based on a mixed weighted criterion combining displacement limitation and material usage minimization into a single objective function. Two scenarios are presented: a) variations in cross-sectional areas, b) variations in both cross-sectional areas and overall truss width.

4.2. General pattern-based approach for frames

This example aims to validate the pattern-based approach for a statically indeterminate frame structure. The implementation leverages an object-oriented methodology, where the frame structure is decomposed into patterns following the general algorithm (Fig. 1). Key structural components, including beams, interfaces, and supports, are represented as objects (Fig. 4). Data exchange between these objects enables to solve both statics and optimization problems.

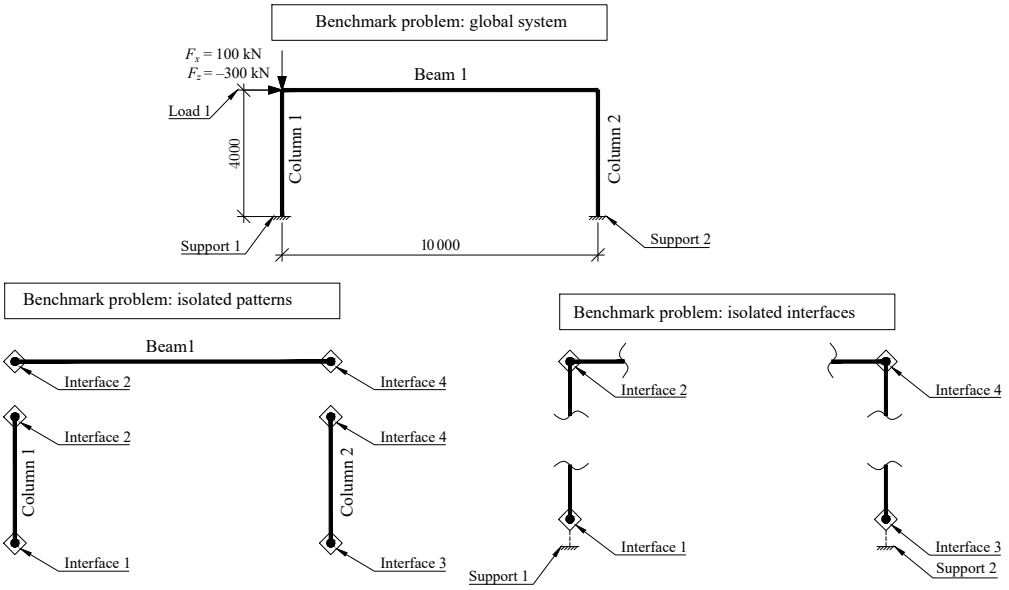

FIG. 4. Scheme of the frame decomposition.

To demonstrate the core principles of the proposed methodology, a simplified benchmark frame was selected to allow for controlled testing and detailed performance evaluation. This setup facilitates a direct comparison between traditional global optimization and the pattern-based decomposition strategy. In particular, we compare the results of full-structure optimization using a genetic algorithm against those obtained via iterative local optimization of individual patterns, all while monitoring interface admissibility criteria and force consistency.

The purpose of this comparative setting is not to outperform classical methods at this stage, but rather to isolate and highlight the inner mechanisms of the pattern-based strategy in a verifiable environment. While promising, the method's competitiveness with established large-scale techniques – such as SIMP-based topology optimization, level-set approaches, or gradient-based shape optimization – requires further research. These classical methods have been validated for highly nonlinear, three-dimensional problems and offer strong theoretical guarantees. Therefore, systematic comparisons in terms of accuracy, robustness, and scalability are deferred to future studies.

To comprehensively evaluate the proposed methodology at the concept stage, three separate benchmark cases were analyzed:

- A global Pareto-based optimization of the full frame structure was conducted to verify the object-oriented framework used for assembling the global stiffness matrix from individual patterns. This analysis investigates how various objective criteria influence the structural configuration and trade-offs between performance and material usage.
- A local iterative optimization of the beam was used to demonstrate the selective recomputation logic. In this case, only the beam cross-section undergoes optimization, while the columns remain fixed. The analysis validates whether the admissibility criteria (Eqs. (17)–(19)) are fulfilled during local stiffness updates without full recalculation.
- A comparative benchmark of recomputation strategies using the genetic algorithm was performed using a modified genetic algorithm. Several scenarios were tested where the global FEM system is recalculated at different intervals (e.g., every 2nd, 5th, or 10th iteration). This benchmark quantifies the trade-off between computational cost and accuracy in a full-structure optimization setting.

The applied loads consist of a vertical concentrated force $F_z = -300$ kN and a horizontal force $F_x = 100$ kN. Two real decision variables are considered, represented as $\mathbf{d} = [S_1 \ S_2]$, where $S_1 \in [200 \ 1000]$ mm is the cross-sectional height of the columns, and $S_2 \in [200 \ 1000]$ mm is the cross-sectional height of the beam. The cross-sectional properties are derived from S_1 and S_2 using approximated values from a selected profile catalogue (HEA profiles).

The optimization considers five criteria:

1. Displacement limitation:

$$F_1(\mathbf{d}) = |h(\mathbf{d}) - h_{\text{adm}}|, \tag{22}$$

where $h_{\text{adm}} = H/500$ and H is the height of the frame.

2. Moment limitation:

$$F_2(\mathbf{d}) = \max_{(\boldsymbol{\xi})} |M(\mathbf{d}, \boldsymbol{\xi})|. \tag{23}$$

3. Longitudinal force limitation:

$$F_3(\mathbf{d}) = \max_{(\boldsymbol{\xi})} |N(\mathbf{d}, \boldsymbol{\xi})|. \tag{24}$$

4. Steel usage minimization: $F_4(\mathbf{d})$ is defined as the total mass of all structural elements, computed according to Eq. (21).

5. Normal stress check:

$$F_5(\mathbf{d}) = \max_{\xi} \left| \frac{1}{f_y} \left| \frac{N(\mathbf{d}, \xi)}{A(\xi)} + \frac{M(\mathbf{d}, \xi)}{W_{\text{pl}}(\xi)} \right| - 0.95 \right|, \tag{25}$$

where $A(\xi)$ is the cross-sectional area, $W_{\text{pl}}(\xi)$ is the plastic section modulus, and $f_y = 235$ MPa is the yield stress.

Here, $\xi \in \mathbb{R}$ represents the scalar physical coordinate corresponding to the local coordinate system attached to a particular bar.

While our optimization framework defines five criteria, each Pareto-optimal analysis only considers a subset of three simultaneously. This approach simplifies interpretation, and allows for meaningful comparison between different trade-off scenarios. For the comparative benchmark of optimization strategies, the mixed objective function combined steel usage (F_4) and stress utilization accuracy (F_5). This allowed for a preliminary basis of comparison across all recomputation strategies.

For benchmarking purposes and to compare local versus global optimization strategies, a modified evolutionary algorithm was implemented. In this approach, global stiffness matrix recomputations are performed only periodically, based on a user-defined interval. The frequency of full FEM recomputation directly influences both computational cost and accuracy. Several scenarios were tested, ranging from a full recalculation at every iteration to more sparse updates (e.g., every 2nd, 3rd, up to 50th iteration).

The object-oriented approach was implemented using C++. The analysis involved 30 finite elements, and a total of 19 600 FEM solutions were performed, corresponding to a 140×140 parameter matrix. The computational time for the

pattern-based approach in C++ was 60 seconds, while the procedural global calculation approach in MATLAB required 1 minute and 22 seconds. These results demonstrate the feasibility and effectiveness of the pattern-based approach for optimizing a simple frame structure, providing a solid foundation for addressing more complex tasks in future implementations.

The optimization results, including all non-dominated solutions and the Pareto front, are depicted in Fig. 5. In these graphs, blue dots represent Pareto-optimal solutions, while gray dots denote non-Pareto solutions. In Fig. 5b, the influence of the axial force criterion on the optimization outcome is minimal, resulting in a Pareto front that appears compressed along the horizontal axis. This reflects the limited contribution of this objective in the given configuration. It is also worth noting that due to the objective-like formulation of the displacement limitation, some Pareto-optimal solutions exhibit $F_1 = 0.678$ m, corresponding to actual displacements significantly exceeding the admissible value. While mathematically non-dominated, such solutions are not acceptable from an engineering standpoint. This issue is illustrated in several entries in Tables 1 and 2, and it highlights a potential drawback of formulating performance targets as objectives instead of enforcing them explicitly through inequality constraints.

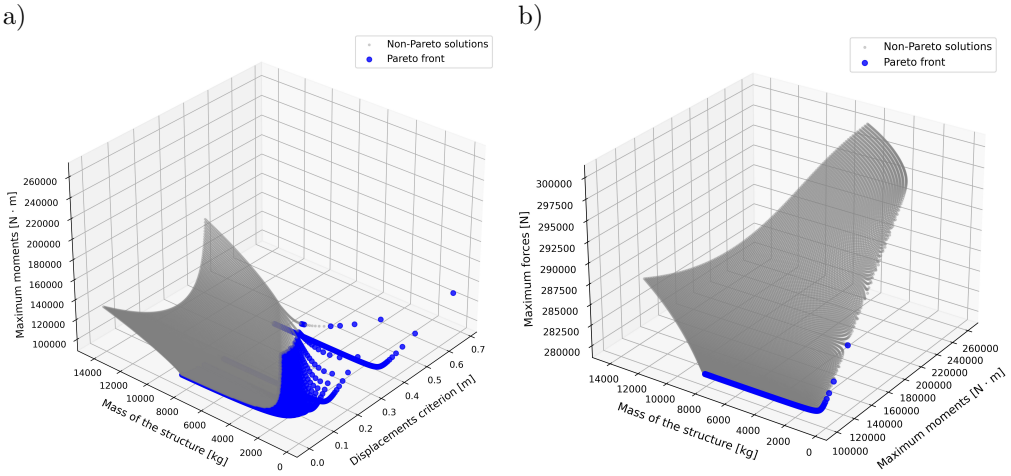

FIG. 5. Graphs illustrating the Pareto optimization results for two scenarios: a) moments criterion with mass and displacement limitations, b) moments and forces criteria with mass limitation.

Preliminary results indicate that, for the considered simple steel frame, it is possible to isolate the beam as a local pattern and perform optimization without the need for global stiffness matrix updates in every iteration. The internal force response, used as the primary admissibility criterion, remained within acceptable bounds even when the surrounding global structure was not fully

Table 1. Representative Pareto-optimal solutions for the three-objective optimization using moments criterion with mass and displacement limitations.

No.	S_1 [mm]	S_2 [mm]	F_1 [m]	F_2 [Nm]	F_4 [kg]
1	100	100	0.678342	129 470	301
2	240	140	0.011220	170 021	729
3	240	450	0.000013	109 625	1882
4	340	200	0.000196	161 372	1263

Table 2. Representative Pareto-optimal solutions for the three-objective optimization using moments and forces criteria with mass limitation.

No.	S_1 [mm]	S_2 [mm]	F_2 [Nm]	F_3 [N]	F_4 [kg]
1	100	100	129 470	285 876	301
2	100	300	100 424	280 079	1017
3	100	600	100 068	280 012	1914
4	100	1000	100 010	279 999	2854

Table 3. Iterative evaluation of admissibility criteria during beam cross-section optimization in the global frame with global displacement limitation.

S_2	F_1 [m]	$\|\mathbf{K}\|$	$\|\mathbf{N}\|$ [N]	$\|\mathbf{V}\|$ [N]	$\|\mathbf{M}\|$ [Nm]	k_x [N/m]	k_y [N/m]	k_θ [Nm/rad]
100	0.678342	1.26E+10	918 813	228 024	358 829	72 927	1.12E+08	439 937
160	0.387504	1.36E+10	902 841	232 026	360 943	129 149	1.12E+08	8.65E+06
220	0.374060	1.59E+10	902 145	232 232	362 305	133 743	1.12E+08	2.12E+07
280	0.369761	1.98E+10	901 926	232 299	362 758	135 273	1.12E+08	3.89E+07
340	0.367775	2.55E+10	901 826	232 329	362 969	135 988	1.12E+08	6.28E+07
400	0.366681	3.29E+10	901 771	232 346	363 086	136 385	1.12E+08	9.48E+07
600	0.365179	6.81E+10	901 697	232 369	363 247	136 931	1.12E+08	3.12E+08
1000	0.364443	1.84E+11	901 660	232 380	363 326	137 200	1.12E+08	2.73E+09

Table 4. Preliminary comparison of global and local optimization approaches for horizontal displacement control in the example steel frame.

Aspect	Global system	Isolated pattern
Stiffness matrix update	Every iteration	Only if Δf exceeds threshold (Eq. (17))
Number of equations to solve in typical iteration (assuming 10 finite elements per column/beam)	93	39
Number of required global FEM solutions (brute force) assuming possible profiles (24 in total) from the HEA catalogue	24	3 (for 1% admissibility threshold)
Optimality	Optimal solution	Sub-optimal solution with deviation within engineering tolerance

recalculated. This is illustrated in the iterative evaluation presented in Table 3. The comparative summary in Table 4 shows that this approach reduced the number of required global finite element analyses, while maintaining a solution within engineering accuracy limits. However, further investigation is needed to confirm whether this strategy applies to more complex structures or different loading and support configurations.

The results, summarized in Table 5, show that reduced recomputation frequencies lead to savings in computational time and the number of global FEM analyses. For instance, switching from full recomputation to recalculating every 5th evaluation reduced the number of global solves from 6060 to 1860, with negligible changes in utilization ratios and weight. Even more intensive reductions (e.g., 1/30 or 1/50) still yielded feasible solutions, although some over- or under-utilization of individual members was observed. The single-objective optimization of the bracing system was performed using the simple genetic algorithm (SGA) implemented in the pagmo2 library. A population size of 60 individuals was used, and the algorithm ran for 100 generations. The optimization involved three real-valued decision variables corresponding to the heights of selected cross-sections. Default tournament selection was applied, and fitness values were evaluated based on a problem-specific weighted objective.

TABLE 5. Comparison of Optimization Strategies (the best ones from 10 GenAlg runs).

Strategy	σ/f_y col. 1	σ/f_y beam	σ/f_y col. 2	Total weight [kg]	No. of recomp.	Time [s]
Full	0.949	0.757	0.937	1831	6060	38
1/2	0.949	0.757	0.937	1831	3329	31
1/3	0.949	0.757	0.937	1831	2532	29
1/4	0.949	0.757	0.937	1831	2204	28
1/5	0.920	0.730	0.921	2055	1860	27
1/10	0.850	0.651	0.922	2104	1373	26
1/20	0.923	0.747	0.959	1911	1293	26
1/30	0.898	0.758	0.885	1991	1114	26
1/50	1.074	0.793	0.951	1407	1086	25

4.3. Vertical bracings configuration

An additional specific type of pattern was analyzed – a vertical bracing layout optimization. The aim of this example is to test optimization approaches for integer-type parameters, where the optimal location of bracings is not known a priori. Although the optimization procedure used here follows a classical, global approach without decomposition, it demonstrates how discrete topological design variables can be incorporated within the pattern-based framework.

The bracing layout is treated as a parameterized pattern that can later be reused in the assembly of more complex structural systems. This example illustrates the framework's capability to address discrete layout decisions, such as selecting and positioning of bracing elements, while maintaining consistency with the modular and extensible nature of the proposed method. For this purpose, the optimization scheme includes limited fixed geometry parameters such as span widths (6 m) and floor heights (3 m), as shown in Fig. 6. The pattern allows for the implementation of restricted areas in where cannot be provided (Fig. 7). For the benchmarks all bracing zones were assumed as allowed, and the test loads were applied to the top right node of the structure. The applied loads consist of a concentrated vertical force $P_1 = -100$ kN and a horizontal force $H_1 = 100$ kN. Four real-type decision variables for cross-sections are taken into account, denoted as $\mathbf{d}_{\text{sections}} = [B \;\; C_1 \;\; C_2 \;\; S]$. The cross-section heights are B, C_1, C_2, $S \in [100 \;\; 1000]$ mm, where B – is the beams cross-section height, C_1, C_2 are columns' cross-section heights, and S is bracings cross-section height. The location and type of bracings are parametrized by using 6×6 matrix of integers representing allowed zones for bracings (Fig. 8), as shown below:

$$\mathbf{d}_{\text{bracings}} = \begin{bmatrix} A_1 & A_2 & \cdots & A_6 \\ A_7 & A_8 & \cdots & A_{12} \\ \vdots & \vdots & \ddots & \vdots \\ A_{31} & A_{32} & \cdots & A_{36}. \end{bmatrix}. \tag{26}$$

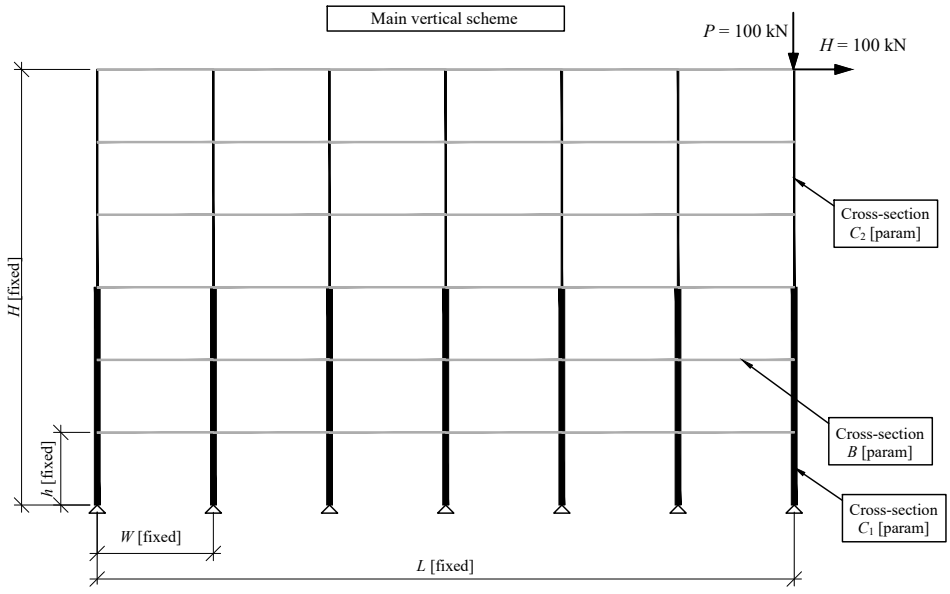

FIG. 6. General scheme.

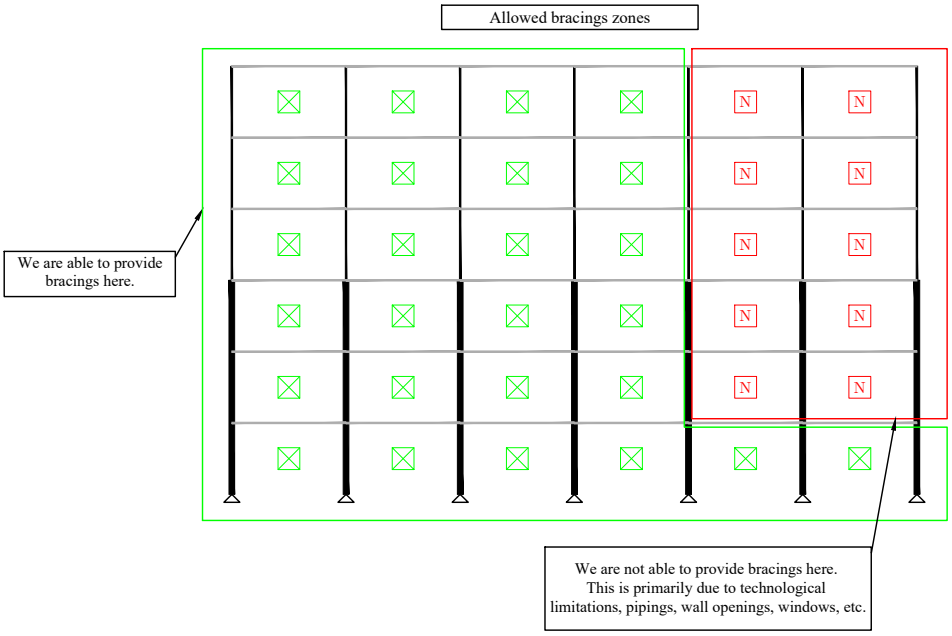

FIG. 7. Allowed and restricted zones based on design limitations.

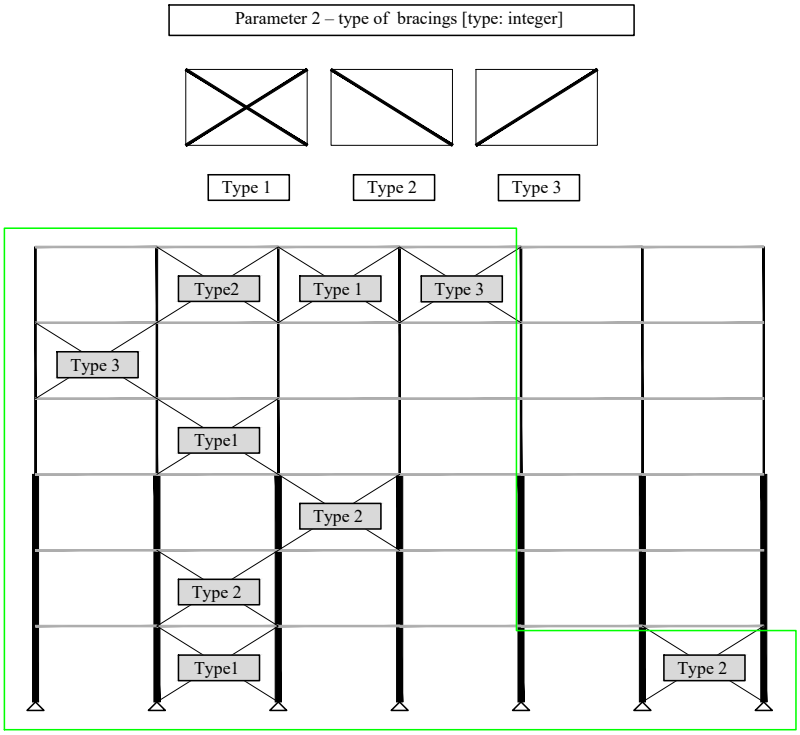

FIG. 8. Parametrization of bracing types.

For benchmarking purposes, five criteria were evaluated:

1. Displacement limitation:

$$F_1(\mathbf{d}) = |h(\mathbf{d}) - h_{\text{adm}}|, \tag{27}$$

where $h_{\text{adm}} = H/500$ (H is the height of the structure).

2. Steel usage minimization: $F_4(\mathbf{d})$ is defined as the total mass of all structural elements, computed according to Eq. (21).
3. Minimization of the number of compressed members:

$$F_3(\mathbf{d}) = \sum_{i=1}^{n_{\text{tot}}} I_{\text{comp}}\big(N_i(\mathbf{d})\big), \tag{28}$$

where

$$I_{\text{comp}}\big(N_i(\mathbf{d})\big) = \begin{cases} 1, & \text{if } N_i(\mathbf{d}) < 0, \\ 0, & \text{otherwise.} \end{cases} \tag{29}$$

In this notation, n_{tot} is the total number of members, and $N_i(\mathbf{d})$ is the axial force in the i-th member. The condition $N_i(\mathbf{d}) < 0$ corresponds to compression.

4. Moment limitation $F_4(\mathbf{d})$, defined as in Eq. (23).
5. Longitudinal force limitation $F_5(\mathbf{d})$, defined as in Eq. (24).

The Pareto front optimization was performed on a frame structure without bracings, while the weighted criteria optimization focused on a complete task

Table 6. Representative Pareto-optimal solutions for the three-objective optimization using moments and forces criteria with mass limitation.

No.	B [mm]	C_1 [mm]	C_2 [mm]	F_5 [N]	F_2 [kg]	F_4 [Nm]
1	100	100	100	56 040	14 991	24 893
2	200	200	280	34 581	61 675	14 817
3	300	300	450	35 466	137 925	14 161
4	500	700	700	34 643	332 306	14 745

Table 7. Representative Pareto-optimal solutions for the three-objective optimization using moments criterion with mass and displacements limitation.

No.	B [mm]	C_1 [mm]	C_2 [mm]	F_1 [m]	F_2 [kg]	F_4 [Nm]
1	100	100	100	0.04403	14 991	56 040
2	100	100	120	0.04440	15 785	34 782
3	120	120	160	0.04639	24 569	34 778
4	140	140	180	0.04674	27 286	34 220

with bracing zones. Although the optimization problem involves five criteria, each Pareto-optimal analysis is limited to three objectives at a time, similarly to the approach used in Subsec. 4.2.

The optimization results, including all non-dominated solutions and the Pareto front, are depicted in Fig. 9. The analysis involved up to 150 finite elements. For the Pareto optimization a total of 19 600 FEM solutions were performed, corresponding to a 140×140 parameter matrix. The computational time was 194 seconds. The single-objective weighted criterion optimization was carried out using the SGA from the pagmo2 library. The optimization process involved a population size of 60 individuals, with the number of generations typically set to 100 or 300, depending on the specific case, as shown in the convergence plots (Figs. 11 and 12). The number of decision variables for this was 40. For the selection process, default tournament selection was used. Fitness values were computed based on a mixed set of criteria, tailored to the specific optimization problem being addressed. The optimization results for the weighted criteria are shown in Fig. 10. Convergence graphs for the genetic algorithm are shown in Figs. 11 and 12. The blue line with circular markers represents the best solution found at each generation, showing how the objective function value improves over iterations. The red line with cross markers depicts the improvement in the objective function between consecutive generations, emphasizing the rate of progress. The first task ran for 100 generations, whereas the second task was executed for 300 generations. The first task, involving 3000 evaluations (FEM solutions), was completed in 26 seconds, whereas the second task, with 9000 evaluations, took 86 seconds. While Figs. 11 and 12 present the convergence

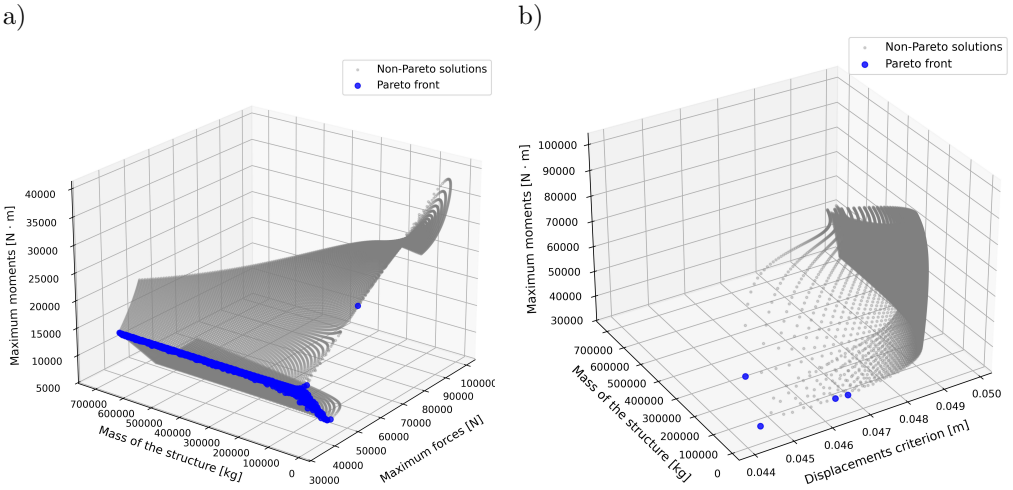

Fig. 9. Graphs illustrating the Pareto optimization results. These graphs show two scenarios: a) moments and forces criteria with mass limitation, b) moments criterion with mass and displacements limitation.

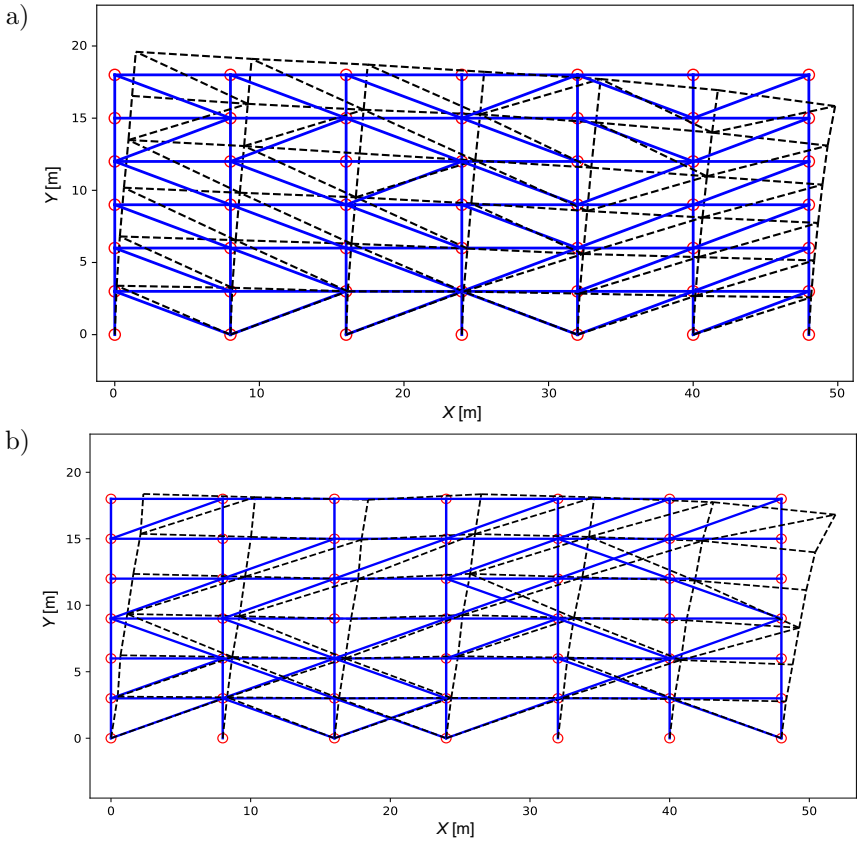

FIG. 10. Graphs illustrating the optimal solutions with deformed configurations for two single-objective functions formulated using mixed criteria: a) a function combining displacement limitation, weight, and the number of compressed members, b) a function combining displacement limitation and weight.

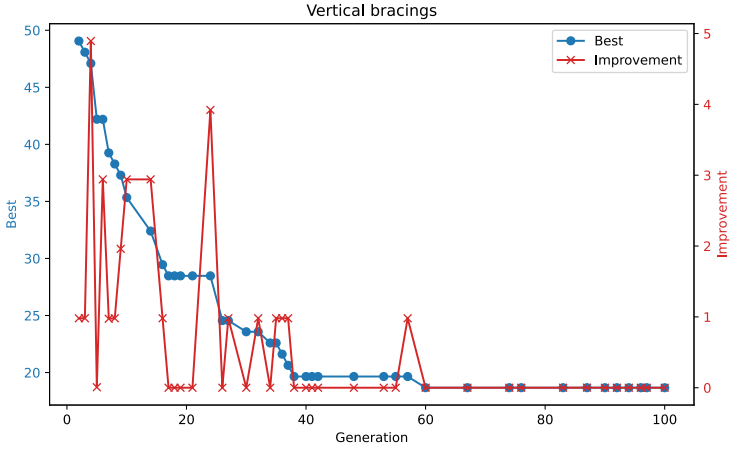

FIG. 11. Convergence graph for the mixed 3 criteria case with 100 generations.

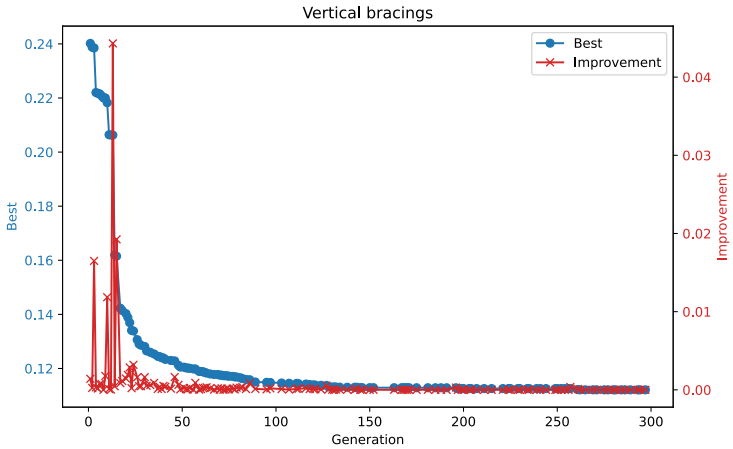

FIG. 12. Convergence graph for the mixed 2 criteria case with 300 generations.

behavior of the optimization process, they do not provide a direct assessment of individual bracing type performance. Due to the mixed-integer nature of the problem, optimal solutions typically comprise combinations of different bracing types. A detailed statistical evaluation of the role of each bracing type was beyond the scope of this study but may be considered in future work.

Based on the obtained results, several conclusions can be drawn: the algorithm effectively identifies optimal solutions within a reasonable time frame, and it successfully combines various types of parameters within a single task. However, some challenges remain: the optimal geometry may not be immediately intuitive for structural designers, complicating the verification process; while the Pareto front provides greater flexibility for designers to select a preferred solution, interpreting results becomes more challenging when dealing with more than three criteria. Additionally, the values on the Pareto front may appear scattered, as shown in Fig. 12b. Moreover, a supplementary algorithm to optimize for multiple load cases is necessary and is planned as part of future research. It should also be emphasized that, similar to the displacement limitation discussed in Subsec. 4.2, certain Pareto-optimal solutions may not satisfy essential engineering requirements despite being mathematically non-dominated. This further supports the need to complement objective-based formulations with explicit constraints to ensure practical applicability.

4.4. Complex frame structure optimization concept

The concept of complex frame decomposition was developed and is illustrated in Fig. 13. This structure integrates various types of patterns and incorporates the parametrization of spring support stiffness (Fig. 14). This example

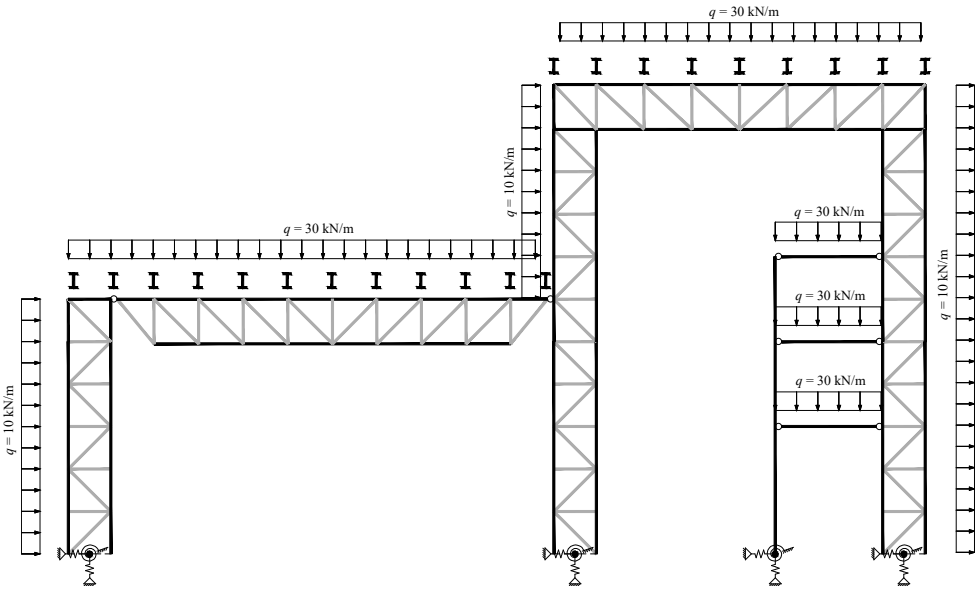

FIG. 13. General scheme of the frame.

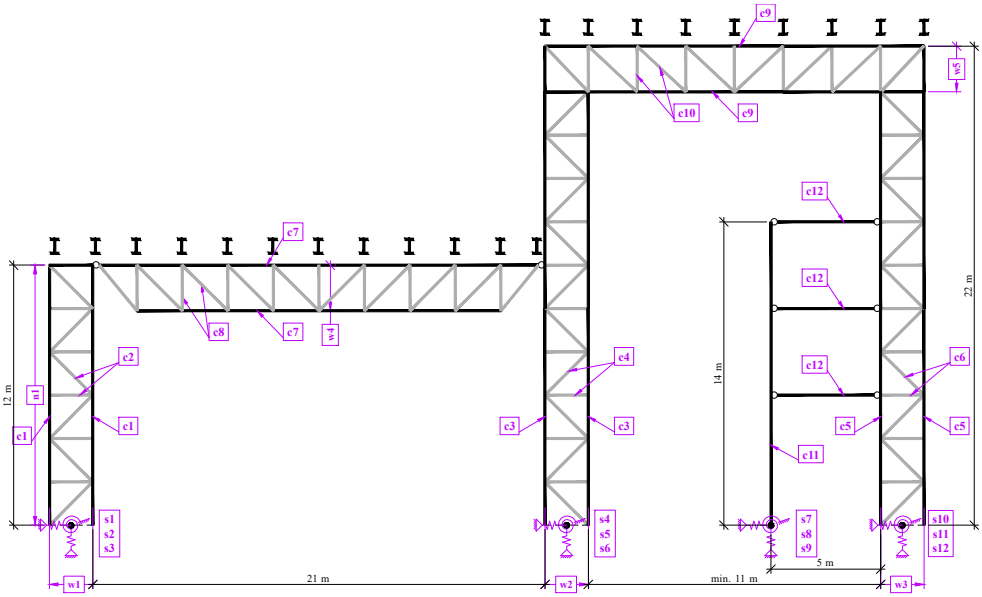

FIG. 14. Parametrization scheme.

serves as an initial step toward a more generalized structural design process in engineering.

The pattern-based approach enables to break down the structure into manageable patterns, facilitating both its assembly and optimization to meet specific

design requirements (Fig. 15). In this case, the decomposition resulted in five truss-type patterns, four beam-type patterns, four spring supports, and 14 interfaces.

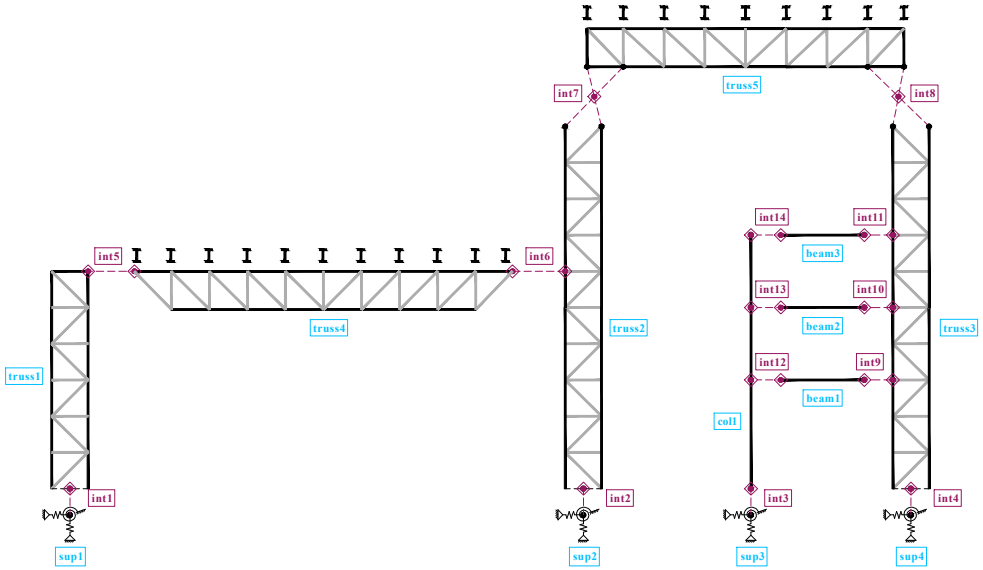

FIG. 15. Decomposition using interfaces.

Additionally, a simplification method employing substitute bar-type elements in the global scheme was explored (Fig. 16). This approach aims to em-

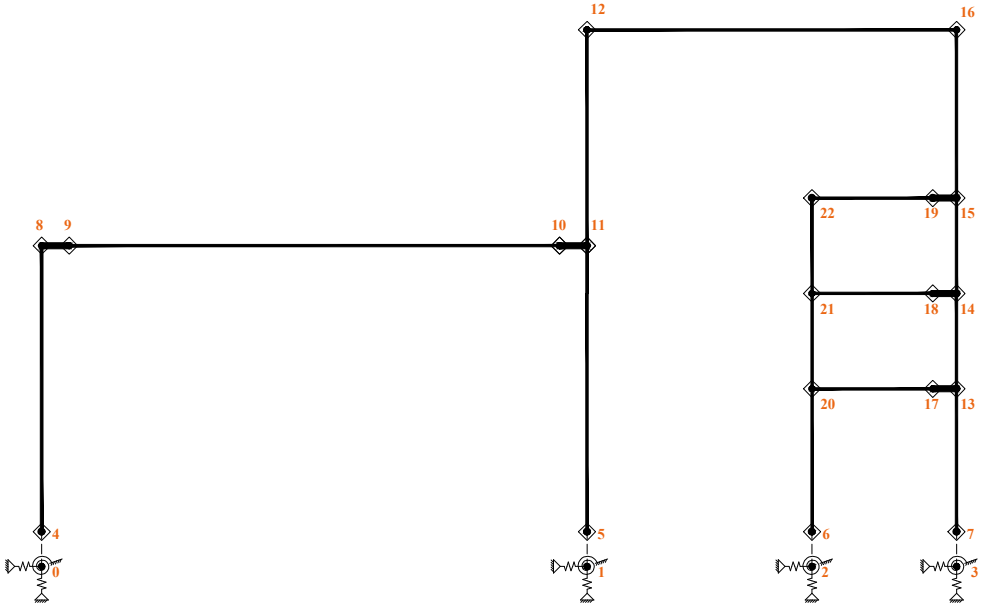

FIG. 16. Simplification of a global scheme by substitute bar-type elements.

ploy a simplified system and reducing the number of finite elements in the global analysis.

Preliminary benchmarks indicate that optimization using the simplified system reduces computational time by 50–60%. This improvement is largely attributed to the reduced number of equations to solve – 27 equations in the simplified system compared to 177 in the full system. While this approach significantly decreases computational demands, its applicability is limited in more general cases. To overcome this limitation, the development of an additional algorithm for detecting connectivity between patterns is necessary. Moreover, the parametrization of spans may require an additional layer of abstraction. Despite these challenges, the approach demonstrates considerable potential for practical applications and merits further investigation.

5. Conclusions

This study – summarizing the second year of a doctoral thesis – advances the pattern-based approach for geometry and topology optimization of steel structures. Primarily, this research focused on developing an interaction-based methodology for pattern-based optimization. It explored optimizing patterns using an object-oriented approach implemented in C++ and investigated the use of spring-type interfaces for connecting patterns. Moreover, results from the global optimization of complex steel structures, combining decision variables of various numerical types, were presented.

Three benchmark problems were analyzed to assess different aspects of the proposed methodology. The first problem involved classical topology optimization with discrete design variants, illustrating how the internal topology of a pattern can be optimized. The second one tested local pattern-based optimization with selective stiffness recomputation, which led to a notable reduction in global FEM evaluations while maintaining acceptable accuracy. The third benchmark addressed a mixed-variable problem, demonstrating the framework's capability to handle discrete layout decisions, such as selecting and positioning of bracing elements. While these findings demonstrate the applicability of the proposed approach in the tested scenarios, they remain limited to a small set of benchmark problems. Therefore, further testing is required to evaluate its performance in more complex or spatial structures.

The proposed pattern-based approach offers several notable advantages. First, it provides individual control over optimality by supporting both global and local optimization. Each pattern can be treated independently, allowing for customized solutions that contribute to greater efficiency and precision in the overall structural design. Second, patterns significantly streamline the decomposition and assembly process. By abstracting structural components into higher-level

entities, the need to manually define finite element models element by element is eliminated, which considerably simplifies the parametrization process. Third, the modular and systematic nature of the approach lays a solid foundation for further development and scalability, enabling its application to increasingly complex and sophisticated engineering problems.

Despite these advantages, several challenges and limitations remain. The additional level of abstraction introduced by pattern-based modeling may not be effective in cases where the structural parametrization is highly specific or inherently complex. This underscores the need for further research and testing. Moreover, in the context of simple structural models, the overhead introduced by the pattern-based framework may outweigh its benefits, resulting in reduced computational efficiency. Finally, for the method to be broadly applicable, a diverse and comprehensive library of structural patterns must be developed, which requires substantial resources and implementation effort.

Future work will focus on optimizing quasi-linear and non-linear problems, especially those involving large deformations. The pattern-based approach will be expanded to accommodate more complex structural designs, with the potential development of a multi-threaded solver (e.g., one thread per pattern). Additional optimization criteria will be explored to increase the approach's applicability. Furthermore, the methodology will be extended to spatial structures, supported by the development of a more sophisticated testing environment in C++ for advanced research and validation.

Acknowledgments

This research is supported by the Polish Ministry of Science and Higher Education under the project DWD/6/0523/2022 "Parameterization of computational models with topology optimization of selected types of building structures".

References

1. G.I.N. Rozvany, Aims, scope, methods, history and unified terminology of computer-aided topology optimization in structural mechanics, *Structural and Multidisciplinary Optimization*, **21**(2): 90–108, 2001, https://doi.org/10.1007/s001580050174.

2. G.I.N. Rozvany, A critical review of established methods of structural topology optimization, *Structural and Multidisciplinary Optimization*, **37**(3): 217–237, 2009, https://doi.org/10.1007/s00158-007-0217-0.

3. O. Sigmund, K. Maute, Topology optimization approaches, *Structural and Multidisciplinary Optimization*, **48**(6): 1031–1055, 2013, https://doi.org/10.1007/s00158-013-0978-6.

4. J. Logo, H. Ismail, Milestones in the 150-year history of topology optimization: A review, *Computer Assisted Methods in Engineering and Science*, **27**(2–3): 97–132, 2020, https://doi.org/10.24423/cames.296.

5. S. Czarnecki, Compliance optimization of the truss structures, *Computer Assisted Methods in Engineering and Science*, **10**(2): 117–137, 2003.

6. F. Yan, Z. Lin, X. Wang, F. Azarmi, K. Sobolev, Evaluation and prediction of bond strength of GFRP-bar reinforced concrete using artificial neural network optimized with genetic algorithm, *Composite Structures*, **161**: 441–452, 2017, https://doi.org/10.1016/j.compstruct.2016.11.068.

7. M. Sonmez, Discrete optimum design of truss structures using artificial bee colony algorithm, *Structural and Multidisciplinary Optimization*, **43**(1): 85–97, 2011, https://doi.org/10.1007/s00158-010-0551-5.

8. M. Papadrakakis, N.D. Lagaros, Reliability-based structural optimization using neural networks and Monte Carlo simulation, *Computer Methods in Applied Mechanics and Engineering*, **191**(32): 3491–3507, 2002, https://doi.org/10.1016/S0045-7825(02)00287-6.

9. D. Jerez, H. Jensen, M. Beer, Reliability-based design optimization of structural systems under stochastic excitation: An overview, *Mechanical Systems and Signal Processing*, **166**: 108397, 2022, https://doi.org/10.1016/j.ymssp.2021.108397.

10. H. Fredricson, Topology optimization of frame structures—joint penalty and material selection, *Structural and Multidisciplinary Optimization*, **30**(3): 193–200, 2005, https://doi.org/10.1007/s00158-005-0515-3.

11. J. Cai, L. Huang, H. Wu, L. Yin, Topology optimization of truss structure under load uncertainty with gradient-free proportional topology optimization method, *Structures*, **58**: 105377, 2023, https://doi.org/10.1016/j.istruc.2023.105377.

12. X. Guo, G.D. Cheng, N. Olhoff, Optimum design of truss topology under buckling constraints, *Structural and Multidisciplinary Optimization*, **30**(3): 169–180, 2005, https://doi.org/10.1007/s00158-004-0511-z.

13. A. Ben-Tal, M.P. Bendsoe, A new method for optimal truss topology design, *SIAM Journal on Optimization*, **3**(2): 322–358, 1993, https://doi.org/10.1137/0803015.

14. E. Croce, E. Ferreira, A. Lemonge, L. Goliatt, H. Barbosa, A genetic algorithm for structural optimization of steel truss roofs, [in:] *XXV Congresso Ibero-Latino Americano de Métodos Computacionais em Engenharia (CILAMCE)*, November, 10–12, Recife, Brasil, 2004.

15. L. Gil, A. Andreu, Shape and cross-section optimisation of a truss structure, *Computers and Structures*, **79**(7): 681–689, 2001, https://doi.org/10.1016/S0045-7949(00)00182-6.

16. B. Etaati *et al.*, Shape and sizing optimisation of space truss structures using a new cooperative coevolutionary-based algorithm, *Results in Engineering*, **21**: 101859, 2024, https://doi.org/10.1016/j.rineng.2024.101859.

17. Y. Lai, Q. Cai, Y. Li, J. Chen, Y.M. Xie, A new evolutionary topology optimization method for truss structures towards practical design applications, *Engineering Structures*, **324**: 119326, 2025, https://doi.org/10.1016/j.engstruct.2024.119326.

18. M. Grzywiński, T. Dede, B. Atmaca, Application of self-adaptive population Rao algorithms to optimization of steel grillage structures, *Computer Assisted Methods in Engineering and Science*, **30**(4): 505–520, 2023, https://doi.org/10.24423/cames.1000.

19. M. Grzywiński, Size and shape design optimization of truss structures using the Jaya algorithm, *Computer Assisted Methods in Engineering and Science*, **27**(2–3): 177–184, 2020, https://doi.org/10.24423/cames.282.

20. Z. Zhao, Z. Kang, T. Zhang, B. Zhao, D. Zhang, R. Yan, Topology optimization algorithm for spatial truss based on numerical inverse hanging method, *Journal of Constructional Steel Research*, **219**: 108764, 2024, https://doi.org/10.1016/j.jcsr.2024.108764.

21. A. Kaveh, S. Talatahari, Optimum design of skeletal structures using imperialist competitive algorithm, *Computers and Structures*, **88**(21): 1220–1229, 2010, https://doi.org/10.1016/j.compstruc.2010.06.011.

22. A. Kaveh, S. Talatahari, Size optimization of space trusses using Big Bang–Big Crunch algorithm, *Computers and Structures*, **87**(17): 1129–1140, 2009, https://doi.org/10.1016/j.compstruc.2009.04.011.

23. A. Kaveh, A. Zaerreza, Reliability-based design optimization of the frame structures using the force method and SORA-DM framework, *Structures*, **45**: 814–827, 2022, https://doi.org/10.1016/j.istruc.2022.09.057.

24. A. Lax, S. Milewski, Advancing computational approaches for geometry optimization of steel structures, *Engineering Transactions*, **72**(2): 159–202, 2024, https://doi.org/10.24423/EngTrans.3223.2024.

25. F. Biscani, D. Izzo, A parallel global multiobjective framework for optimization: pagmo, *Journal of Open Source Software*, **5**(53): 2338, 2020, https://doi.org/10.21105/joss.02338.

26. S. Timoshenko, J. Gere, *Theory of Elastic Stability*, 2nd ed., Dover Civil and Mechanical Engineering, Dover Publications, 2012.

Received January 15, 2025; revised version May 16, 2025;
accepted June 9, 2025; published online June 26, 2025.